Exploring L1 syndrome-causing L1CAM as a trans-synaptic modulator of mGluR5

by

Sarah Cameron

A thesis submitted to the Department of Biological Sciences, University of Manitoba,
in partial fulfilment of the requirements for the course

BIOL 4100

for the degree of

Bachelor of Science (Honours)

Abstract

Neurotransmission typically occurs when neurotransmitters, released by the presynapse, interact with receptors on the postsynapse. Interruptions in these interactions can lead to neurological disorders. Recently, these trans-synaptic interactions were found to involve synaptic adhesion molecules, modulating the activity of a subgroup of G protein-coupled receptors (GPCRs) known as the metabotropic glutamate receptors (mGluRs). A synaptic adhesion molecule called L1CAM has been found to interact with mGluR5. L1CAM is of particular interest because it is the known cause of L1 syndrome, a neurodevelopmental disorder that can cause hydrocephalus, spastic paraplegia, and intellectual disability. As a well-established drug target for neurological disorders, mGluR5, in complex with L1CAM, may have major implications in the etiology of L1 syndrome. We hypothesize that L1CAM is a trans-synaptic modulator of mGluR5. Co-immunoprecipitation experiments were conducted to detect binding of L1CAM, the synaptic adhesion molecule, to the receptors, mGluR5 and mGluR2 (a negative control), at the protein level. Trans-cellular signaling experiments were conducted to determine the functional response of the L1CAM-mGluR interaction at the cellular level. As a result, we found that L1CAM does complex with mGluR5 and not mGluR2. A functional response has not yet been seen, but it is possible that different experimental conditions are required to accurately reflect cell conditions *in vivo*. In future research, discovery of L1CAM-mGluR5 trans-cellular modulation would lead to further understanding of trans-synaptic interactions between mGluRs and synaptic adhesion molecules, and possibly further the understanding of the etiology of L1 syndrome. As an overarching objective of possible L1CAM-mGluR5 modulation, a therapeutic could be developed to rescue the interaction of L1CAM and mGluR5 in those with L1 syndrome.

Acknowledgments

I would like to acknowledge everyone who has made this academic journey possible. First, I would like to thank my supervisor, Henry Dunn, for providing longstanding support and mentorship throughout my time in his lab. I would like to thank all of my fellow students in the lab for their kind, positive attitudes and advice throughout the writing process, as well as for training me, particularly Sam Laurencelle, Simran Dhaliwal, Simrat Dhaliwal, and Kaden Baskerville. I would like to thank my committee, including Lei Xing, Paul Marcogliese, and Joy Stacey, for providing new insight into my research project, and challenging me to think outside the box, encouraging my growth as a researcher.

This research would not have been possible without lab funding and support from St. Boniface Hospital Research, Excellence in Neurodevelopment and Rehabilitation Research In Child Health (ENRRICH), Natural Sciences and Engineering Research Council of Canada (NSERC), Research Manitoba, BioTalent Canada, and Brain Canada Foundation. Additionally, BioRender was used to create a diagram for this thesis, as labelled with "Created with BioRender.com" in the caption.

Finally, I would like to thank everyone else who supported me, by listening to me practice my presentations, getting me coffee, and overall cheering me on, including my parents, Lori Bunio-Cameron and James Cameron, as well as Gage Cameron, Dylan Nickel, Joce Blanco, Lukas Lam, Obaid Maqsood, Hanna Spring and Abby Spring. You have all played a part in my biggest project to date, and I sincerely hope we never stop returning these favours.

Table of Contents

List of Figures

Introduction

Neurotransmission is the basis for all communication occurring in the brain and nervous system, yet many protein interactions involved in synaptic communication remain poorly understood. Characterizing synaptic interactions is crucial for understanding the mechanisms of neurotransmission. Synaptic interactions involving receptors can lead to modulation of neuronal signaling (Feng et al. 2001; Dunn et al. 2018; Sun et al. 2005). G protein-coupled receptors (GPCRs) are highly involved in neuronal signaling, as they are the target of 33% of approved small molecule drugs (Santos et al. 2017). Fascinatingly, GPCRs have recently been found to form trans-synaptic complexes with synaptic adhesion molecules (Boucard et al. 2014; Dunn et al. 2018; Silva et al. 2011), with neuromodulation particularly occurring in a subset of GPCRs called metabotropic glutamate receptors (mGluRs) (Dunn et al. 2018; Dunn et al. 2019). The discovery of trans-synaptic modulation between mGluRs and synaptic adhesion molecules represents a new possible direction for therapeutics (Dunn et al. 2018).

mGluRs are organized into three groups (I, II, and III) based on sequence homology and pharmacology (Dhami et al. 2006; Dunn et al. 2018; Trivedi et al. 2012). Within a group, mGluRs share approximately 70% sequence similarity, while between groups, there is approximately 45% sequence similarity (Conn and Pin 1997). Sequence similarity within a group is related to receptor coupling to G-proteins (Conn and Pin 1997). Group I mGluRs (mGluR1 and mGluR5) are coupled to the $G\alpha_q$ G-protein, and are located primarily on the post-synapse, where they respond to glutamate inputs from the pre-synapse (Dhami et al. 2006; Dunn et al. 2018). Group II (mGluR2 and mGluR3) and

Group III (mGluR4, mGluR6, mGluR7 and mGluR8) are coupled to the $G\alpha_{i/o}$ G-protein, and primarily located on the pre-synapse where they are involved in neurotransmitter release (Dunn et al. 2018).

Of all eight mGluRs, mGluR5 has had the most success in drug-related clinical trials (Pillai et al. 2016). Several mGluR5-regulating drugs have reached phase II clinical trials, suggesting mGluR5 may be a viable target for therapeutic design (Pillai et al. 2016). Using immunoprecipitation and mass spectrometry, potential binding partners of mGluR5 have been identified (Farr et al. 2004). L1 cell adhesion molecule (L1CAM) was identified as a binding partner (Farr et al. 2004), and is of particular interest as a synaptic adhesion molecule. Mutations in the L1CAM gene are the known cause of L1 syndrome, a neurodevelopmental disorder (Christaller et al. 2017; Marín et al. 2015; Wang et al. 2022). L1 syndrome comprises a family of X-linked recessive neurological disorders, though it may be referred to as a single disorder with several varying phenotypes (Christaller et al. 2017; Marín et al. 2015; Vos et al. 2010). The four phenotypes typically seen in patients are (1) hydrocephalus due to stenosis of the aqueduct of Sylvius (HSAS), (2) mental/intellectual disability, aphasia, shuffling gait, and adducted thumbs (MASA) syndrome, (3) spastic paraplegia, and (4) agenesis of the corpus callosum (Marín et al. 2015; Vos et al. 2010). Phenotypes can appear together or separately, and vary in severity between patients (Lyonnet et al. 1992). L1 syndrome ranges from lethal phenotype occurring prenatally or at birth (typically in patients with the HSAS phenotype) to a mild-to-moderate phenotype, where patients often reach adulthood (Lyonnet et al. 1992; Vos et al. 2010).

The severity of the phenotype depends on the type of mutation: truncating mutations in the ectodomain of L1CAM lead to a more severe phenotype (hydrocephalus and abnormal neurogenesis, increased intellectual disability, and early death), while missense mutations in the ectodomain lead to a moderate phenotype (normal neurogenesis and physical brain development, some intellectual disability) (Fransen et al. 1998; Otter et al. 2017; Vos et al. 2010; Yamasaki et al. 1997). The ectodomain of L1CAM makes up the majority of the protein, being approximately 200 kilodaltons (kDa) and having six Ig-like domains next to five fibronectin type III domains (Kiefel et al. 2012; Yamasaki et al. 1997). The ectodomain is followed by a single-pass transmembrane domain (32 kDa) and a small cytoplasmic domain (13 kDa) (Kiefel et al. 2012; Yamasaki et al. 1997). All cytoplasmic mutations in L1CAM lead to less severe phenotypes than mutations in the ectodomain (Fransen et al. 1998; Yamasaki et al. 1997).

As a synaptic adhesion molecule and identified potential binding partner of mGluR5, L1CAM has the potential to modulate mGluR5 signalling. As a result, it is possible that any mutations in L1CAM may disrupt this interaction with mGluR5, and may be involved in the phenotypic changes seen in patients with L1 syndrome. We hypothesize that L1CAM is a trans-synaptic modulator of mGluR5, in that it causes a change in mGluR5 signaling activity. Our first research objective is to establish mGluR5 as a binding partner of L1CAM, and establish mGluR2 as a negative control for L1CAM signaling experiments. mGluR5 differs from mGluR2 in that mGluR5 is primarily expressed on the postsynaptic terminal while mGluR2 is primarily expressed on the presynaptic terminal, and the ectodomain sequence of mGluR2 is the most dissimilar from that of mGluR5 (Jin et al. 2017; Piers et al. 2012), so we consider it the best mGluR

to test for a negative control. Our second objective is to characterize the function of L1CAM as a modulator of mGluR5 pharmacology through optimization of a signaling assay, in comparison to the negative control.

Methods and Materials

Cell culture

Human embryonic kidney 293 (HEK-293) cells were maintained by regularly passaging cells into culture dishes, growing in Dulbecco's Modified Eagle Medium (DMEM) supplemented with fetal bovine serum, nonessential amino acids, sodium pyruvate, streptomycin, and penicillin. Cells were stored in an incubator at 37°C with 5% CO_2. Depending on the experiment, cells were passaged into 10-centimeter dishes (for co-immunoprecipitation) or 6-centimeter dishes (for cell signalling).

Transfection

For any experiment, cells were passaged ~24 hours before transfection. Cells were transfected at approximately 70% confluency (as the cells must be actively dividing for efficient transfection, and cell division is less active when there are too many cells in the plate), in DMEM with the above supplements excluding the antibiotics (penicillin and streptomycin). This is to avoid excess antibiotics from entering the cell as it is endocytosing, as this would lead to cytotoxicity and possibly cell death. Cells were transiently transfected with double-stranded plasmid DNA using polyethylenimine (PEI), a cationic polymer. In separate tubes, plasmid DNA and PEI were diluted using Opti-MEM™, at a ratio of 3:1. The PEI and DNA were then mixed and incubated for 10-20 minutes, to allow complexes to form. The PEI-DNA complexes were added to cells, and cells were incubated at 37°C for 24 hours.

Ectodomain expression

The ectodomain of L1CAM (tagged with Fc, and will further be referred to as L1CAM-Fc in this section) was transiently transfected into cells as previously described. The media was replaced with Opti-MEM™ 6 hours after transfection, and the plate was placed back into the incubator. The L1CAM-Fc protein was secreted from the cells, into the Opti-MEM™. After 48 hours, the Opti-MEM™ was harvested, protease inhibitor was added, and the solution was stored in the -80°C freezer.

Co-immunoprecipitation

Co-immunoprecipitation experiments were used to qualitatively test whether mGluR5 and mGluR2 bind to L1CAM when tested in the same experiment. In each co-immunoprecipitation experiment, a 10-centimeter plate of cells was transfected with 15 ug of mGluR5- or mGluR2-expressing plasmid DNA and incubated at 37°C for approximately 24 hours. Cells were harvested with phosphate-buffered saline (PBS), and lysed using lysis buffer containing 4% protease inhibitor. Lysate and co-immunoprecipitation samples were made by combining mGluR5 or mGluR2 proteins with L1CAM-Fc proteins or the Fc tag, using lysis buffer to equalize volumes. 20 uL of β mercaptoethanol-containing sample buffer was added to the lysate samples, and stored in the -20°C freezer, and co-immunoprecipitation samples complexed while rotating in the cold room at 4°C for approximately 20 hours. A plate of non-transfected cells at approximately 90% confluency was harvested, lysed, and added to protein G Dynabeads, as a pre-clearing measure. After 20 hours, pre-cleared Dynabeads were washed using lysis buffer at room temperature, and were then added to each co-immunoprecipitation sample. Co-immunoprecipitation samples with Dynabeads complexed on the rotator in the cold

room at 4°C for approximately 1 hour. Using a strong magnet, Dynabead-protein complexes were moved to the side of each tube, and the cell protein-containing solution was aspirated. Co-immunoprecipitation samples were washed with lysis buffer approximately 5 times. 35 uL of β mercaptoethanol-containing sample buffer was added to the co-immunoprecipitation samples to elute the protein complexes from the beads.

The western blotting technique was used to identify proteins within the protein complexes. Sodium dodecyl sulfate-polyacrylamide gel electrophoresis (SDS-PAGE) was conducted to separate the proteins by molecular mass, referenced by molecular protein ladders. After gel electrophoresis, the proteins were transferred to a solid medium (polyvinylidene difluoride membrane) by the wet transfer method, where the gel and the membrane were lined up directly beside one another in a tank filled with transfer buffer, and proteins were electrophoretically transferred on to the membrane. Blocking buffer (10% milk powder in Tris-Buffered Saline with Tween (TBS-T)) was then applied to the membrane for 30 minutes, to inhibit nonspecific binding of antibodies. Primary antibodies specific to each protein in the samples were applied to the membrane for approximately 20 hours. The membrane was washed with TBS-T, then secondary antibody (specific to the primary antibody) was applied to the membrane for 1 hour. The secondary antibody is labelled with horseradish peroxidase, which reacts with an enhanced chemiluminescence substrate and emits light at 425 nm. This light was captured by the Bio-Rad ChemiDoc™ Imager that can detect this chemiluminescence. Proteins appeared in the image as dark bands at the expected mass.

Co-immunoprecipitation statistical analysis

In co-immunoprecipitation experiments, the experimental unit represents one experiment, through cell culturing, transfection, lysing, and the western blotting process. Each experiment was completed with a different passage of HEK-293 cells, to ensure independence. Co-immunoprecipitation experiments are qualitative, in that we were measuring whether the protein is present or not. The lysate samples represent control conditions, as they ensure proper transfection and antibody function.

mGluR5 Optimization with ONE-GO

In the mGluR5 optimization experiment, 6-centimeter plates of cells were transfected with 5 ug of plasmid DNA and incubated at 37°C for approximately 24 hours. We tested different ratios of ONE vector G protein Optical (ONE-GO) biosensor DNA to mGluR5 DNA (1:2, 1:4, 1:6, 1:12) to determine the optimal ratio for signalling activity detection. Each condition was co-transfected with increasing volumes of mGluR5 (as described by the ratios), equal volumes of ONE-GO biosensor, and pcDNA was used to equalize DNA amounts. Each ratio was tested in the presence or absence of a glutamate transporter, excitatory amino acid transporter 3 (EAAT3), due to the high constitutive activity of mGluR5. The mGluR5 optimization protocol after transfection is identical to the following trans-cellular signalling protocol, except cells expressing pcDNA or L1CAM will not be added.

Trans-cellular signaling

Trans-cellular signalling experiments quantitatively measured the mGluR activity in mGluR5- and mGluR2-expressing cells. In each trans-cellular signalling experiment, 6-

centimeter plates of cells were transfected with 5 ug of plasmid DNA and incubated at 37°C for approximately 24 hours. Each condition was co-transfected with ONE-GO biosensor and either mGluR5, mGluR2, or pcDNA. The transfected ONE-GO biosensor includes a Gα subunit tagged with yellow fluorescent protein (YFP) and nanoluciferase, a luminescent enzyme, fused with a detector molecule that detects a GTP-Gα complex. The 1:12 and 1:2 ratios of the biosensor to mGluR was based on the results of the optimization of mGluR5 with ONE-GO. Separate plates were transfected with 5 ug of pcDNA or L1CAM. Approximately 24 hours after transfection, cells were harvested with PBS and centrifuged at 500 x g for 5 minutes at room temperature. The PBS was aspirated and replaced by 1 mL of Hanks' Balanced Salt Solution (HBSS), the pelleted cells were resuspended by pipetting, and centrifuged at 500 x g for 5 minutes at room temperature. This wash was repeated 3 times. Cells were resuspended in 600 uL HBSS. Cells expressing ONE-GO and either mGluR5, mGluR2, or pcDNA were plated in a white 96 well plate, and cells expressing pcDNA or L1CAM were added at a 1:2 ratio. In subsequent experiments, a 1:4 ratio was used, so cells expressing pcDNA or L1CAM were resuspended in 300 uL HBSS to double the number of cells per unit volume, ensuring equality in volume per well across experiments. Cells were co-cultured in an incubator at 37°C for 1 hour. The cells were then incubated in the plate reader for 30 minutes to allow for acclimation to the change in gas composition, then the plate was immediately inserted into the plate reader (BioTek Synergy Neo2), to incubate at 37°C and atmospheric CO_2 for 30 minutes. The plate reader injected cells with Promega Nano-Glo Luciferase Assay Substrate, which reacted with nanoluciferase, an enzyme that produces an intense blue (460 nm) luminescence. After 30 seconds, 1.4 mM glutamate

was injected into the well containing cells, for a final glutamate concentration of ~300μM. This activated the GPCR (mGluR5 or mGluR2) causing the YFP-fused Gα protein to swap GDP for GTP and dissociate from the receptor. Gα-GTP then came in close contact (<10 nm) with the nanoluciferase, fused with a detector molecule with a high specificity for Gα-GTP but not Gα-GDP. This proximity allowed light emission from nanoluciferase to excite YFP, causing it to produce an intense yellow (540 nm) luminescence. Therefore, an increase in yellow light represents increased mGluR activation. The plate reader measured these interactions as wavelengths of light from nanoluciferase and YFP, then bioluminescence resonance energy transfer (BRET) ratios (540nm/460nm) were calculated.

Trans-cellular signalling statistical analysis

mGluR activation was calculated as the change in BRET ratio following glutamate injection. GPCR-biosensor cells co-cultured with pcDNA-expressing cells represent the control treatment, and represent the baseline for characterizing any change in GPCR-biosensor cells co-cultured with L1CAM-expressing cells. Changes in BRET ratio over time were normalized to the maximum value of the corresponding control condition, and calculated as a percentage of the control, such that the maximum value is represented as 100%. Change in BRET ratio over time was represented using a line graph. The change in BRET ratio was quantified by averaging the last 5 reads of the transcellular assay for each condition, as these reads have allowed for the most time for stabilization of the signal after glutamate injection. To normalize data between experiments, the average change in BRET ratio of each condition was divided by the mean value of the averages of its respective control from each experiment. For example, in an experiment where n=3, if A,

B, and C are average values of the last 5 reads of the control (pcDNA-expressing cells) condition, and X, Y, and Z are average values for the experimental (L1CAM-expressing cells) condition, A, B, and C were individually divided by the mean of A, B and C, and X, Y and Z were individually divided by the mean of A, B, and C. The resulting values represent signaling activation as a percent of a condition's control values. Statistical tests were performed using GraphPad Prism software, to compare the change in BRET ratio of each condition (as a percent of the control) with pcDNA-expressing cells added or L1CAM-expressing cells added. Shapiro-Wilk normality tests were applied. If the data was normal, we used a parametric unpaired t-test, and if the data was non-normal, we would use an unpaired, nonparametric t-test, specifically the Mann-Whitney U test.

Results

The L1CAM ectodomain interacts with mGluR5, and not mGluR2, at the protein level (Figures 1, 2, and 3). Since L1CAM has been reported to bind to mGluR5 via immunoprecipitation (Farr et al. 2014), we started by establishing that the L1CAM ectodomain binds to mGluR5, concurrently establishing that the L1CAM ectodomain does not bind to mGluR2, via co-immunoprecipitation experiments. L1CAM-Fc was secreted from HEK293 cells, and allowed to complex with the lysates of separate cells expressing mGluR5 or mGluR2. The co-immunoprecipitation experiments revealed that the ectodomain of L1CAM does indeed bind to mGluR5, and not mGluR2, shown in immunoprecipitation blots immunoblotted (IB) with primary mGluR5 or mGluR2 antibody (Figures 1, 2, and 3). To ensure that the L1CAM ectodomain, and not the Fc tag, of L1CAM-Fc was forming these interactions, the Fc tag itself was used as a control. As shown in the left lane in IB:mGluR5 and IB:mGluR2 immunoprecipitation blots, the Fc tag was unable to pull out both mGluR5 and mGluR2 (Figures 1, 2, and 3). These experiments identify mGluR5 as a binding partner, and mGluR2 as a negative control, of the ectodomain of L1CAM.

Activation of mGluR5 via ONE-GO is best optimized at a DNA transfection ratio of 1:12 (ONE-GO:mGluR5) in the presence of EAAT3 (Figures 4 and 5). Cells were co-transfected with different DNA ratios of ONE-GO biosensor to mGluR5 (1:2, 1:4, 1:6, 1:12), in the presence and absence of transfected EAAT3 DNA. The cells were injected with 1.4 mM glutamate, activating mGluR5 and causing excitation of YFP, leading to the emission of 540 nm wavelengths of light (Figure 6). BRET ratios were calculated between the 540 nm light emitted from YFP and the 460 nm light emitted from

nanoluciferase (540nm/460nm) for each optimization condition. BRET values were averaged for each technical replicate, then normalized to the last 5 seconds before glutamate injection, and plotted (Figure 4). The condition that included a 1:12 DNA ratio of ONE-GO to mGluR5 in the presence of EAAT3 had the highest average BRET values at all time points after glutamate injection (30.0s) (Figure 4). All conditions that included mGluR5 and EAAT3 had a much higher response than conditions without EAAT3 (Figure 4). Analysis of the normalized BRET values of each technical replicate revealed a degree of overlap in response level between conditions with both mGluR5 and EAAT3, particularly between 1:12 and 1:2 (Figure 5). For this reason, transcellular signalling experiments were conducted using both 1:12 and 1:2 ratios, with EAAT3.

L1CAM does not yet appear to modulate mGluR5 pharmacology (Figures 7, 8, 9, and 10). At the 1:2 cell ratio of pcDNA- and L1CAM-expressing cells, both the 1:12 (Figure 7) and 1:2 (Figure 8) DNA ratio of ONE-GO to mGluR, activation levels of mGluR5 are visibly similar over time (Figure 7a and 8a). There is not a significant difference in the change in BRET ratio (represented as a percent of control) at the 1:12 DNA ratio nor the 1:2 DNA ratio when mGluR5-expressing cells are exposed to pcDNA- or L1CAM-expressing cells (both passed Shapiro-Wilk normality tests; unpaired t-tests) (Figure 7b and 8b). mGluR2-expressing cells were exposed to L1CAM-expressing cells and pcDNA-expressing used as a control measure, as we have established that mGluR2 does not bind to L1CAM. As expected, activation levels of mGluR2 are visibly similar over time in pcDNA and L1CAM conditions (Figure 7c and 8c), and mGluR2 did not have a significant difference in the change in BRET ratio at the 1:12 DNA ratio (passed Shapiro-Wilk normality test; unpaired t-test) nor the 1:2 DNA ratio (did not pass Shapiro-

Wilk normality test; Mann-Whitney U-test) when mGluR2-expressing cells were exposed to pcDNA- or L1CAM-expressing cells (Figure 7d and 8d). Similar results were observed at the 1:4 cell ratio of pcDNA- and L1CAM-expressing cells (Figure 9 and 10). In both the 1:12 (Figure 9) and 1:2 (Figure 10) DNA ratio of ONE-GO to mGluR, activation levels of mGluR5 (Figure 9a and 10a) and mGluR2 (Figure 9c and 10c) are visibly similar over time. There was not a significant difference in the change in BRET ratio in mGluR5 at the 1:12 DNA ratio (passed Shapiro-Wilk normality test; unpaired t-test) (Figure 9b), mGluR5 at the 1:2 DNA ratio (did not pass Shapiro-Wilk normality test; Mann-Whitney U-test) (Figure 10b), mGluR2 at the 1:12 ratio (passed Shapiro-Wilk normality test; unpaired t-test) (Figure 9d), and mGluR2 at the 1:2 ratio (passed Shapiro-Wilk normality test; unpaired t-test) (Figure 10d).

Discussion

We established a binding interaction between L1CAM and mGluR5, and consequently established that there is not an interaction between L1CAM and mGluR2 (n=3) (Figures 1, 2, and 3). The full-length L1CAM protein has previously been identified as a potential binding partner of mGluR5, through co-immunoprecipitation of rat brain lysates (Farr et al. 2004). By incubating the L1CAM ectodomain with mGluR5-expressing HEK-293 cell lysates, we further demonstrated that 1) the interaction exists when expressed using HEK-293 cells, and 2) it is the ectodomain of L1CAM that is interacting with mGluR5. mGluR5 is known to complex with other molecules that cause a change in its signalling activity (Beraldo et al. 2016; Um et al. 2013). Group I mGluRs, including mGluR5, have been identified interacting with prion protein (PrP^C) (Beraldo et al. 2011; Um et al. 2013). It has been suggested through these findings that PrP^C acts as an extracellular scaffolding protein, to enable a complex of multiple proteins to form with group I mGluRs (Beraldo et al. 2016; Martins et al. 2010). mGluR5-PrP^C complexes bind to laminin, a glycoprotein, and this interaction modulates signalling pathways involved in memory and neuronal plasticity (Beraldo et al. 2011). mGluR5-PrP^C complexes also bind to β-amyloid oligomers (AβOs), and this interaction is linked to Alzheimer's disease as it modulates pathways involved in disruption of synaptic homeostasis, leading to excitotoxicity, and finally neuronal death (Beraldo et al. 2016; Laurén et al. 2009; Um et al. 2013). A phase I drug trial is ongoing for a drug that disrupts the interaction between AβO-bound PrP^Cs and mGluR5 (Alzheimer's Drug Discovery Foundation, 2014; Haas et al. 2017). These studies show that extracellular binding partners of mGluR5 can have profound effects on its signalling activity and major impacts on the overall neural health of an individual. Further, they demonstrate how maladaptive interactions can be

prevented through the development of a therapeutic that targets the interaction. If L1CAM modulates mGluR5 activity, it is possible that mutations in L1CAM disrupt this interaction, leading to downstream effects which may be involved in L1 syndrome. As opposed to preventing an interaction, such as between AβO-bound PrP^Cs and mGluR5, a therapeutic could be developed to simulate the binding of L1CAM and mGluR5, rescuing the interaction.

All transcellular assays with ratios of ONE-GO to mGluR (1:2, 1:4, 1:6, and 1:12) with EAAT3 had increased signalling activity compared to their counterparts without EAAT3 (Figure 4). This is likely because EAAT3 acts as a regulator for glutamate uptake (Stachowicz et al. 2021). Glutamate is the major excitatory neurotransmitter released by neurons, and the most common free amino acid in the brain (Stachowicz et al. 2021; Zhou et al. 2014). Excessive glutamate in the synapse can cause excitotoxicity, a phenomenon where cell death can occur due to overexcitation of glutamate receptors (Malik et al. 2019; Zhou et al. 2014). mGluR5 prevents overexcitation by rapid endocytosis after interacting with glutamate (Fourgeaud et al. 2003; Trivedi and Bhattacharyya, 2012). Interestingly, mGluR5 internalization can also occur in the absence of glutamate (Fourgeaud et al. 2003; Trivedi and Bhattacharyya, 2012). After endocytosis, mGluR5 receptors are recycled back to the membrane after 3.5 hours (Trivedi and Bhattacharyya, 2012). Due to the constitutive internalization of mGluR5, it may become desensitized more easily than other receptors (Trivedi and Bhattacharyya, 2012). For this reason, we transfected EAAT3 into the HEK293 cells, which removes the glutamate from the extracellular environment and may prevent a degree of glutamate-dependent internalization of the mGluR5 receptors prior to experimental glutamate injection. Cells

can naturally leak out glutamate, which may be activating and desensitizing mGluR5 receptors in cells in the same well in a 96-well plate. By transfecting all cells with EAAT3, the leaked glutamate may be uptaken back into the cells, rather than interacting with mGluR5 receptors on the plasma membrane. Our results suggest that EAAT3 does play a role in preventing densensitization of mGluR5 before the experimental glutamate injection takes place.

Our results do not show that L1CAM modulates mGluR5 signalling activity (Figure 7, 8, 9 and 10). There was no significant change in BRET ratio between administration of pcDNA- and L1CAM-expressing cells to mGluR5-expressing cells at both the 1:2 and 1:4 cell ratio, for both the 1:12 and 1:2 ONE-GO to mGluR DNA ratios. If L1CAM were to show modulation of mGluR5, we would expect a deviation between the data points of the traces showing the change in BRET ratio over time, and a significant difference in the change in BRET ratio. This type of mGluR modulation by a cell adhesion molecule has been shown with ELFN1 modulating the activity of all group III mGluRs (mGluR4, mGluR6, mGluR7, and mGluR8) (Dunn et al. 2018). Specifically, group III mGluR-expressing cells exposed to ELFN1-expressing cells had a significantly decreased change in BRET ratio, representing decreased G-protein activation (Dunn et al. 2018). Functionally, ELFN1 acts as a negative allosteric modulator by binding to mGluRs and causing a conformational change, decreasing the efficacy (activation of the receptor) and by decreasing the affinity of agonists to the receptor, as shown by an increased half maximal effective concentration for L-glutamic acid when exposed to ELFN1-expressing cells (Christopher et al. 2015; Dunn et al. 2018). ELFN1 selectively modulates group III mGluRs, and does not interact with group I and group II mGluRs (Dunn et al. 2018).

mGluR group-based interaction selectivity is not limited to ELFN1 – as previously mentioned, PrP^C selectively interacts with group I mGluRs and is involved in facilitating modulation (Beraldo et al. 2016; Martins et al. 2010). If further research shows that L1CAM does modulate mGluR5, mGluR1 should also be investigated to detect possible group I mGluR selectivity of L1CAM.

It is possible that the transcellular signaling assay protocol has not yet been optimized to accurately reflect modulation of mGluR5 by L1CAM that occurs *in vivo*. An example of a change made to the protocol during this study was the addition of a 30 minute incubation in the plate reader, to allow the cells to acclimate to the change in gas composition between the incubator and plate reader, as the cells would not necessarily be reacting to an environmental change when efficiently signalling *in vivo*. Additionally, both the 1:2 and 1:4 mGluR- to L1CAM-expressing cell ratios were tested here, but it is possible that a higher ratio is required, so that theoretically more mGluRs are able to find and interact with L1CAM proteins in the assay. It is possible that other changes should be made, such as using a different approach than expression of L1CAM in live cells – instead, soluble ectodomain fragments of L1CAM could be delivered to mGluR5-expressing cells (Silva et al. 2011). This strategy has been used to show the induction of Ca^{2+} signaling when latrophilin 1, a GPCR, is exposed to purified ectodomain fragments of a teneurin-2 splice variant (a cell-cell adhesion receptor) (Jackson et al. 2018; Silva et al. 2011). It is possible that this ectodomain purification and delivery technique could facilitate interactions between L1CAM and mGluR5 more efficiently than in co-culture.

As of the end of this study, we have successfully established that the L1CAM ectodomain binds to mGluR5 and not mGluR2, a 1:12 DNA ratio of ONE-GO biosensor

to mGluR5 is optimal for capturing the signalling activity though a 1:2 DNA ratio is interestingly a close second, and the signalling activity of mGluR5 is stronger in the presence of EAAT3. It is still unclear as to why 1:12 and 1:2 ONE-GO to mGluR DNA ratios have a similar effect on mGluR5 signaling compared to the 1:4 and 1:6 DNA ratios, and it is still unclear whether L1CAM modulates mGluR5 signaling activity. Goals for the future of this project should include increasing the number of replicates of signalling assays, altering L1CAM- and mGluR5- expressing cell ratios to explore optimization of the protocol, and testing out new assay methods such as L1CAM ectodomain purification and administration to mGluR5-expressing cells (Dunn et al. 2018; Silva et al. 2011).

Further research into the interaction of L1CAM and mGluR5 may be critical for elucidating disrupted molecular pathways individuals with L1 syndrome. The characterization of a functional modulation response between L1CAM and mGluR5 could lead to further research on pathogenic mutations for L1 syndrome, to test whether the L1CAM-mGluR5 functional response is disrupted (Christaller et al. 2017; Marín et al. 2015). If L1CAM allosterically modulates mGluR5, it is possible that a therapeutic could be developed to act as an alternative allosteric modulator of mGluR5 in patients with mutations in L1CAM (Dunn et al. 2018). The revelation of a pharmaceutical target for L1 syndrome that may allow a rescue of disrupted signaling activity would be a major advancement in the study of L1 syndrome, and has potential to improve quality of life for those affected.

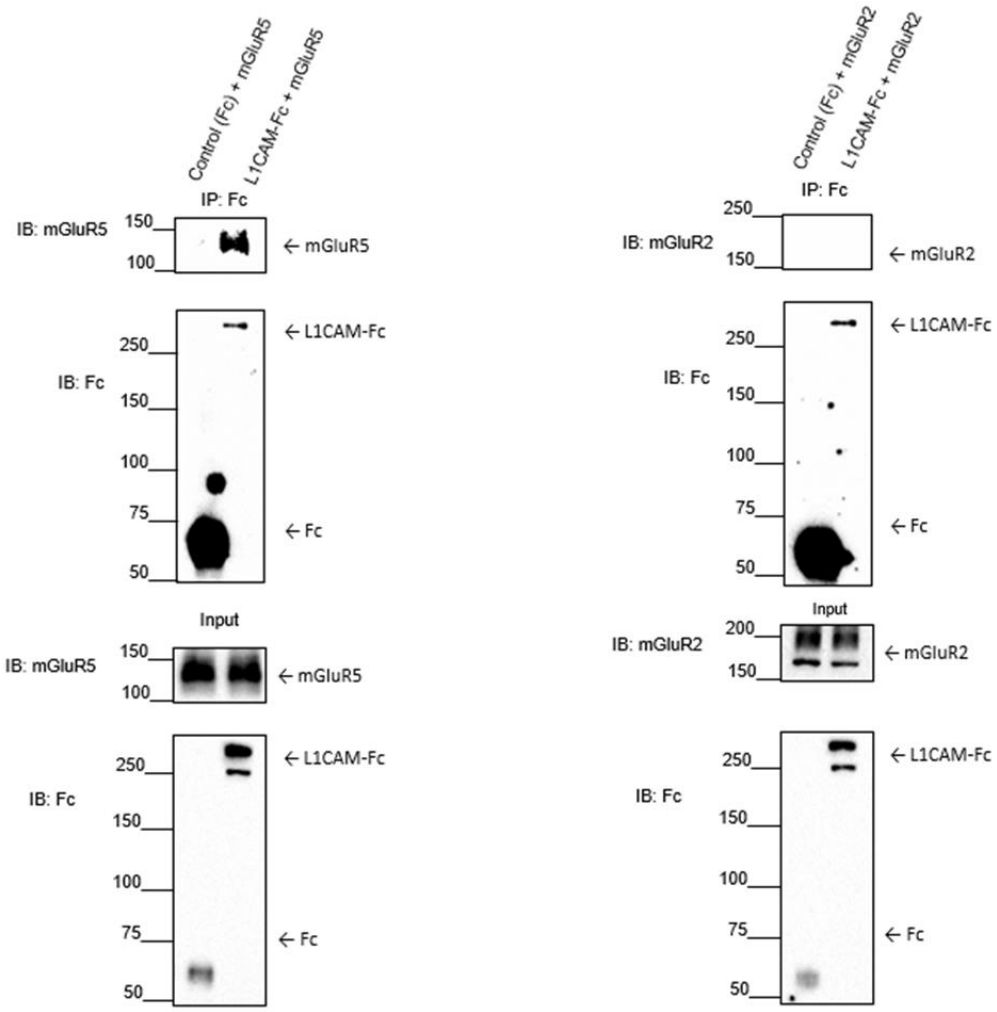

Figure 1. Replicate 1 of co-immunoprecipitation experiments, between L1CAM-Fc and mGluR5 (left) and L1CAM-Fc and mGluR2 (right). Fc is used as a control in both mGluR5 and mGluR2 experiments. The left lane in all blots represents the control lane, containing only the Fc tag and the mGluR. The right lane represents the experimental lane, containing L1CAM-Fc and the mGluR. The top two blots for each experiment represent the immunoprecipitated (IP) samples. The bottom two blots for each experiment represent the lysate (input) samples, used as a control measure to ensure antibody function and to compare to the mass of immunoprecipitated proteins. The primary antibody used for each blot is indicated to the left of the image (IB = immunoblotted).

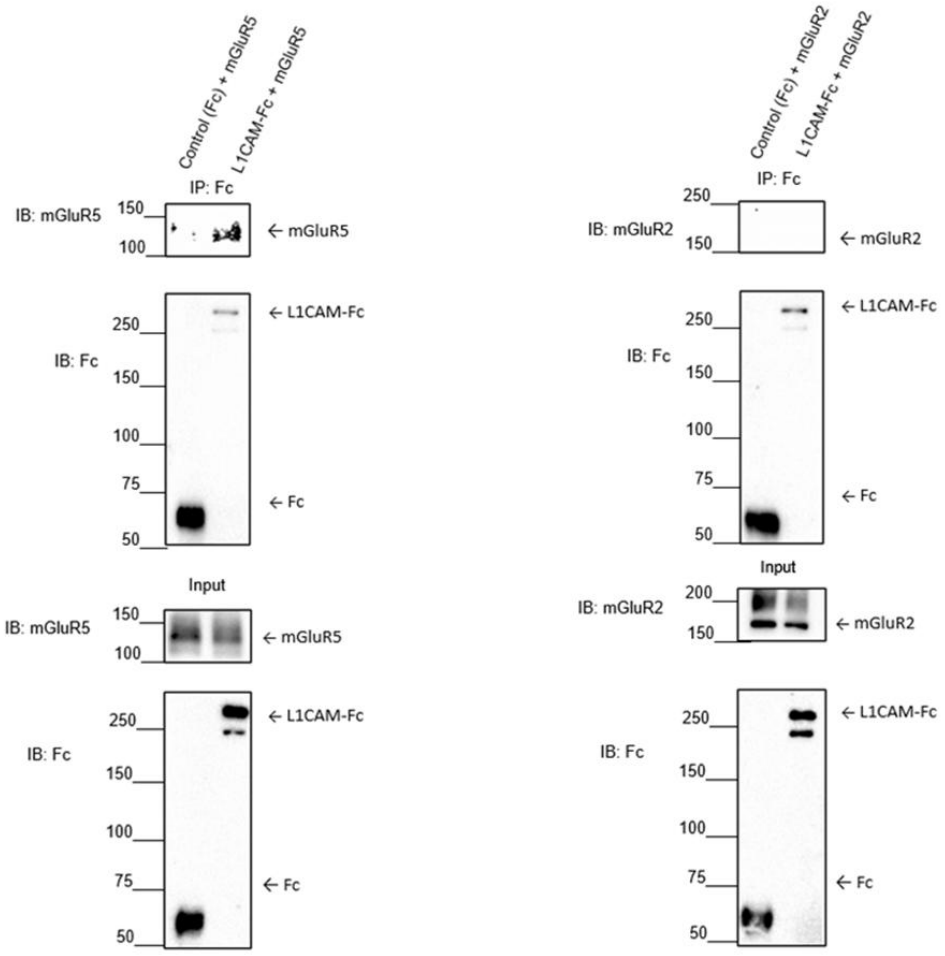

Figure 2. Replicate 2 of co-immunoprecipitation experiments, between L1CAM-Fc and mGluR5 (left) and L1CAM-Fc and mGluR2 (right). Fc is used as a control in both mGluR5 and mGluR2 experiments. The left lane in all blots represents the control lane, containing only the Fc tag and the mGluR. The right lane represents the experimental lane, containing L1CAM-Fc and the mGluR. The top two blots for each experiment represent the immunoprecipitated (IP) samples. The bottom two blots for each experiment represent the lysate (input) samples, used as a control measure to ensure antibody function and to compare to the mass of immunoprecipitated proteins. The primary antibody used for each blot is indicated to the left of the image (IB = immunoblotted).

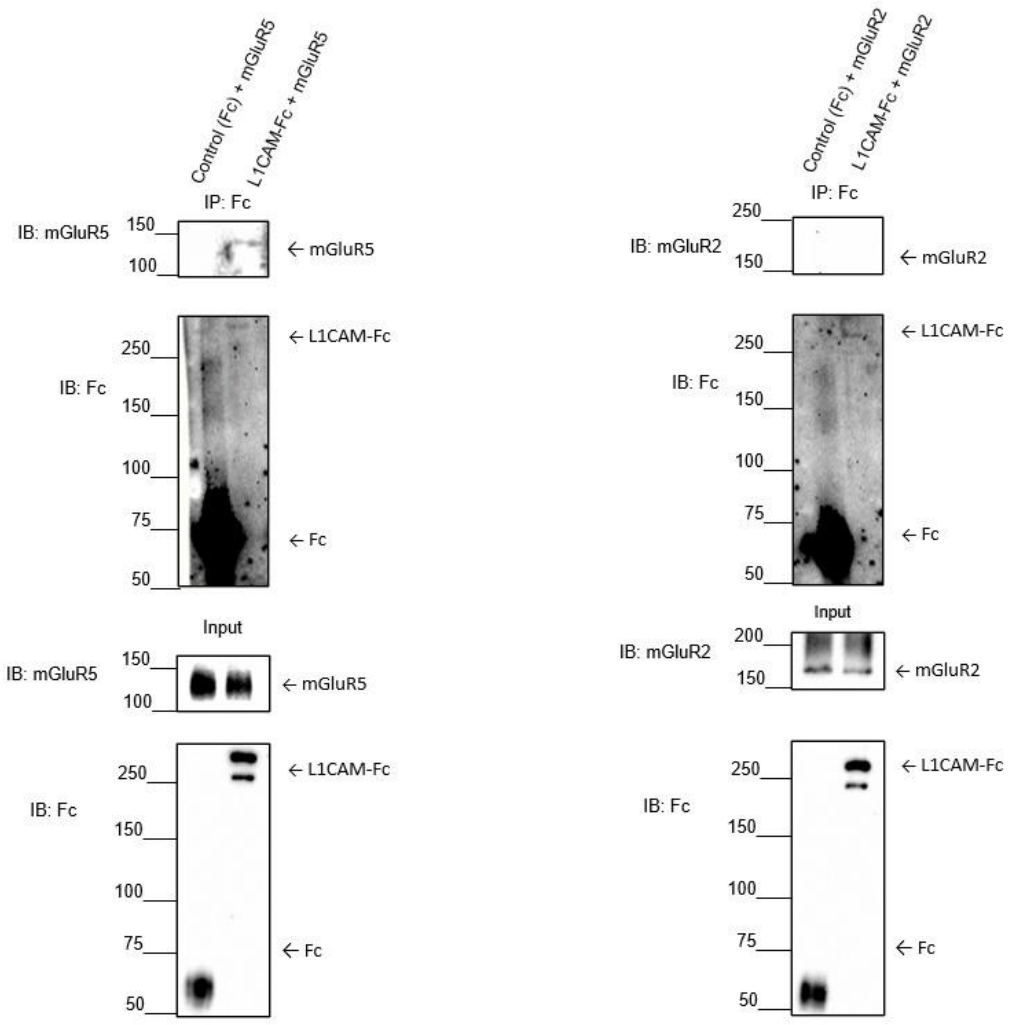

Figure 3. Replicate 3 of co-immunoprecipitation experiments, between L1CAM-Fc and mGluR5 (left) and L1CAM-Fc and mGluR2 (right). Fc is used as a control in both mGluR5 and mGluR2 experiments. The left lane in all blots represents the control lane, containing only the Fc tag and the mGluR. The right lane represents the experimental lane, containing L1CAM-Fc and the mGluR. The top two blots for each experiment represent the immunoprecipitated (IP) samples. The bottom two blots for each experiment represent the lysate (input) samples, used as a control measure to ensure antibody function and to compare to the mass of immunoprecipitated proteins. The primary antibody used for each blot is indicated to the left of the image (IB = immunoblotted).

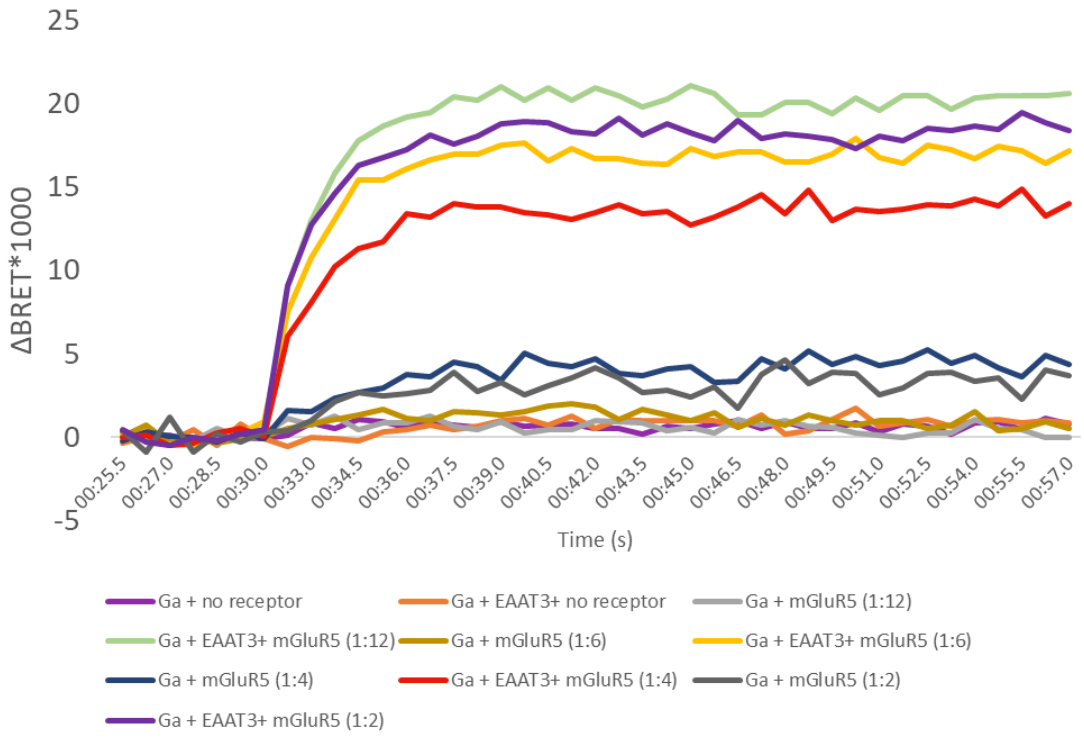

Figure 4. Change in BRET ratios for 10 different conditions, normalized to the last 5 seconds before glutamate injection, which occurs at 30.0s. Conditions include cells transfected with 1:2, 1:4, 1:6, and 1:12 ratios of ONE-GO biosensor to mGluR5, in the presence and absence of transfected EAAT3 DNA. Conditions with ONE-GO and no receptor, in the presence and absence of EAAT3, are included as a control measure to ensure low baseline activity of ONE-GO in the absence of an mGluR.

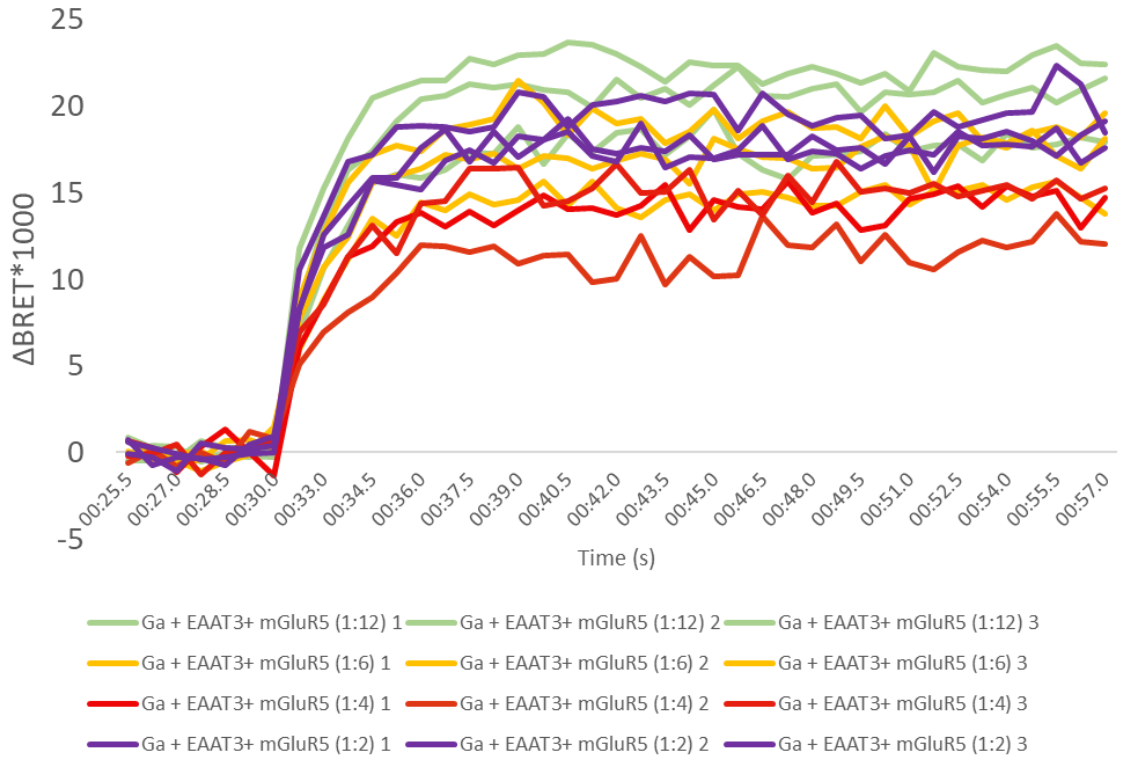

Figure 5. Change in BRET ratios for each technical replicate of 1:2, 1:4, 1:6, and 1:12 conditions of ONE-GO biosensor to mGluR5, in the presence of EAAT3, normalized to the last 5 seconds before glutamate injection (at 30.0s).

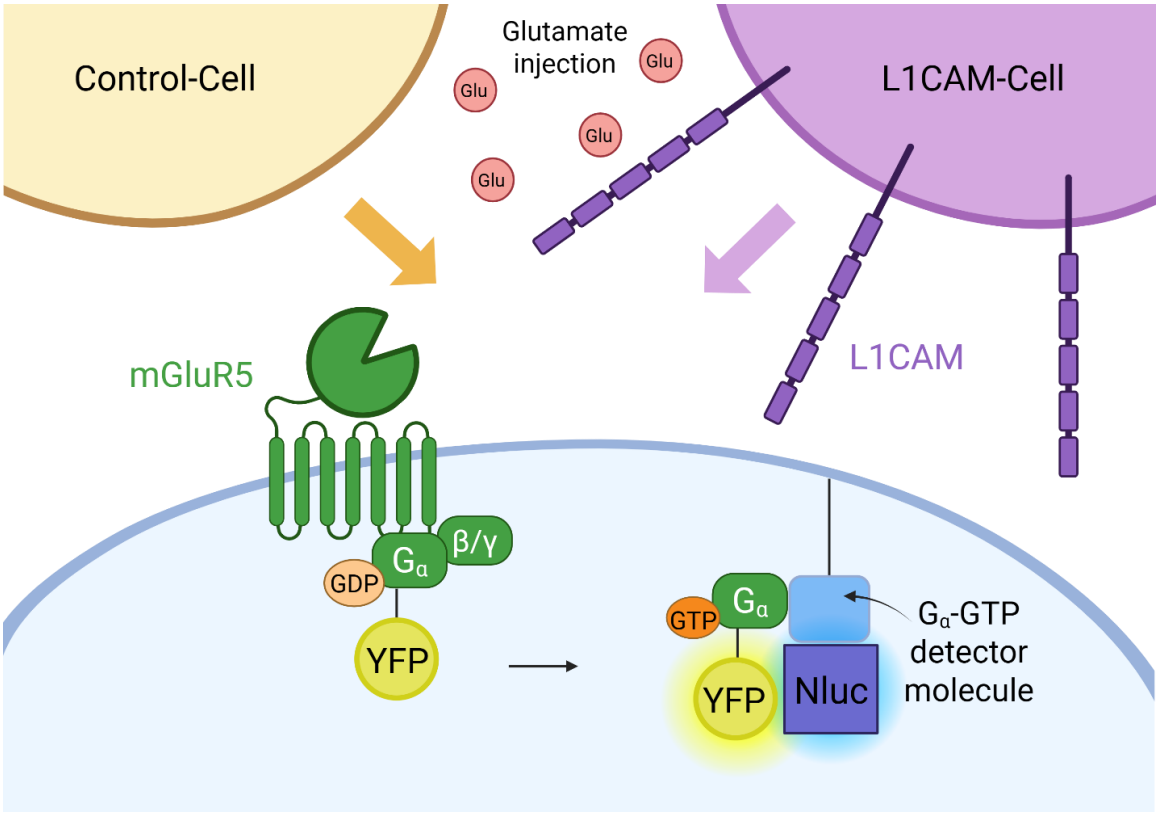

Figure 6. Visual representation of the BRET-based cell signalling assay. Glutamate is injected into the well, stimulating signalling activity in cells expressing an mGluR. mGluR5-expressing cells are co-cultured with cells expressing either pcDNA or L1CAM, to identify if L1CAM has a modulatory effect on mGluR5 signalling activity. When an mGluR is activated by glutamate, it causes YFP-fused Gα protein to swap GDP for GTP and dissociate from the receptor. The Gα-GTP then comes in close contact with the nanoluciferase, fused to a detector molecule that has a high specificity for Gα-GTP. Light emission from nanoluciferase excites YFP, causing it to produce an intense yellow luminescence (540 nm). The yellow light represents mGluR activation, which is later calculated as a ratio to the blue light emission (460 nm) by nanoluciferase. Created with BioRender.com.

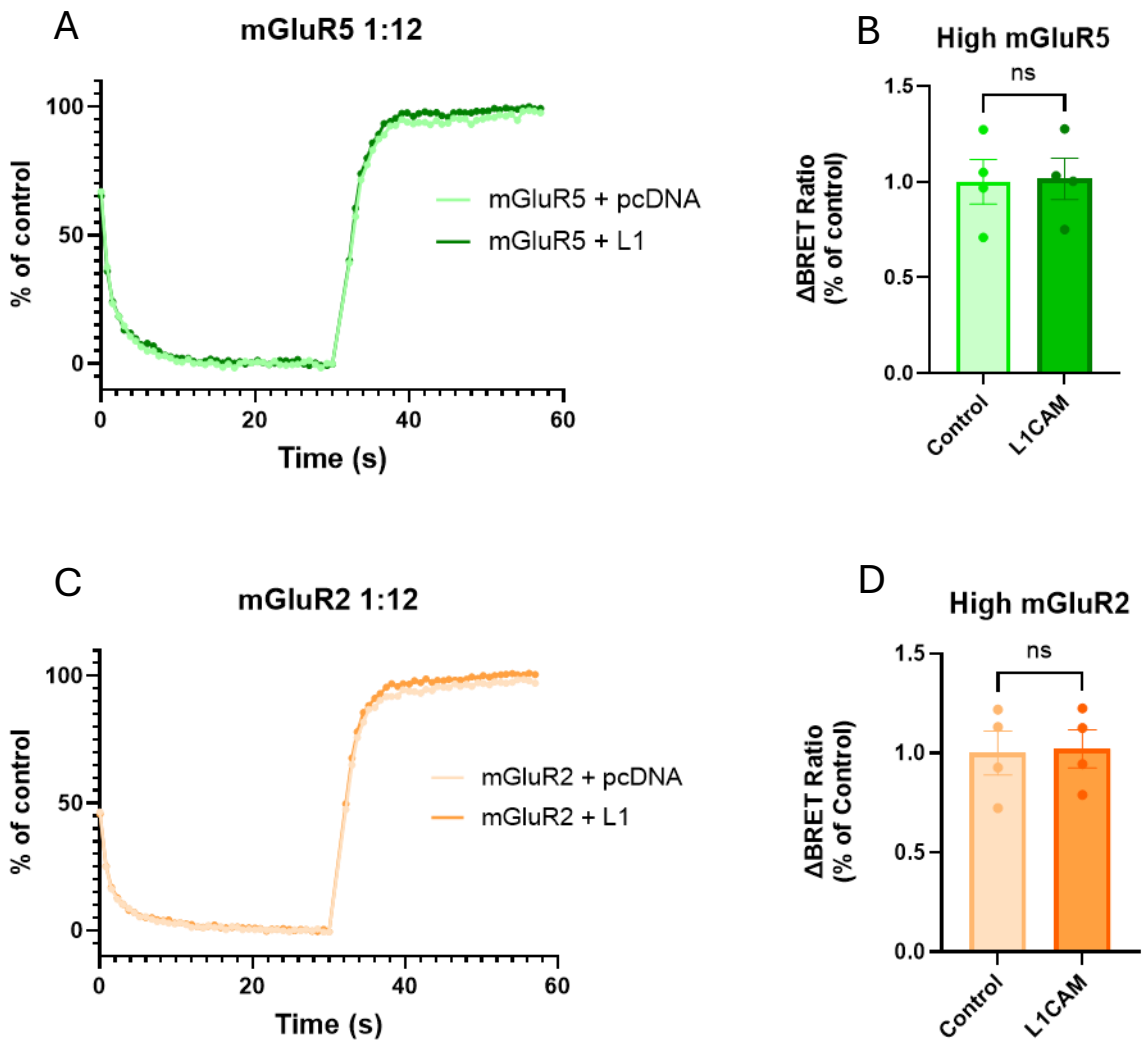

Figure 7. Transcellular interactions between mGluR- and L1CAM-expressing cells at a 1:2 cell ratio, with pcDNA-expressing cells as a control, at the 1:12 DNA ratio of ONE-GO to receptor (n=4). A) Change in BRET ratios between mGluR5-expressing cells cocultured with pcDNA- or L1CAM-expressing cells, calculated as a percent of the control over time. Glutamate injection occurred at 30.0s. B) Quantification of the change in BRET ratio of mGluR5 activation (unpaired t-test). C) Change in BRET ratios between mGluR2-expressing cells cocultured with pcDNA- or L1CAM-expressing cells. D) Quantification of the change in BRET ratio of mGluR2 activation (unpaired t-test).

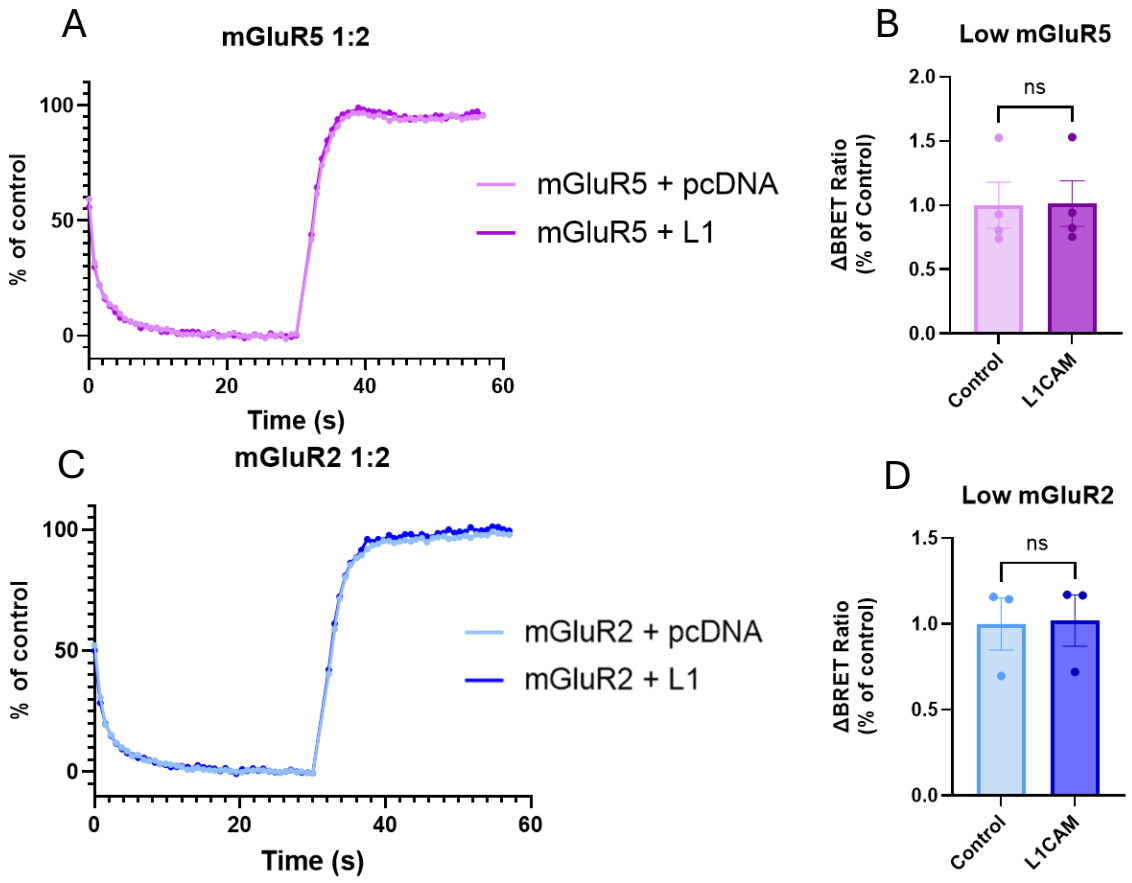

Figure 8. Transcellular interactions between mGluR- and L1CAM-expressing cells at a 1:2 cell ratio, with pcDNA-expressing cells as a control, at the 1:2 DNA ratio of ONE-GO to receptor (n=4 for mGluR5, n=3 for mGluR2). A) Change in BRET ratios between mGluR5-expressing cells cocultured with pcDNA- or L1CAM-expressing cells, calculated as a percent of the control over time. Glutamate injection occurred at 30.0s. B) Quantification of the change in BRET ratio of mGluR5 activation (unpaired t-test). C) Change in BRET ratios between mGluR2-expressing cells cocultured with pcDNA- or L1CAM-expressing cells. D) Quantification of the change in BRET ratio of mGluR2 activation (Mann-Whitney U-test).

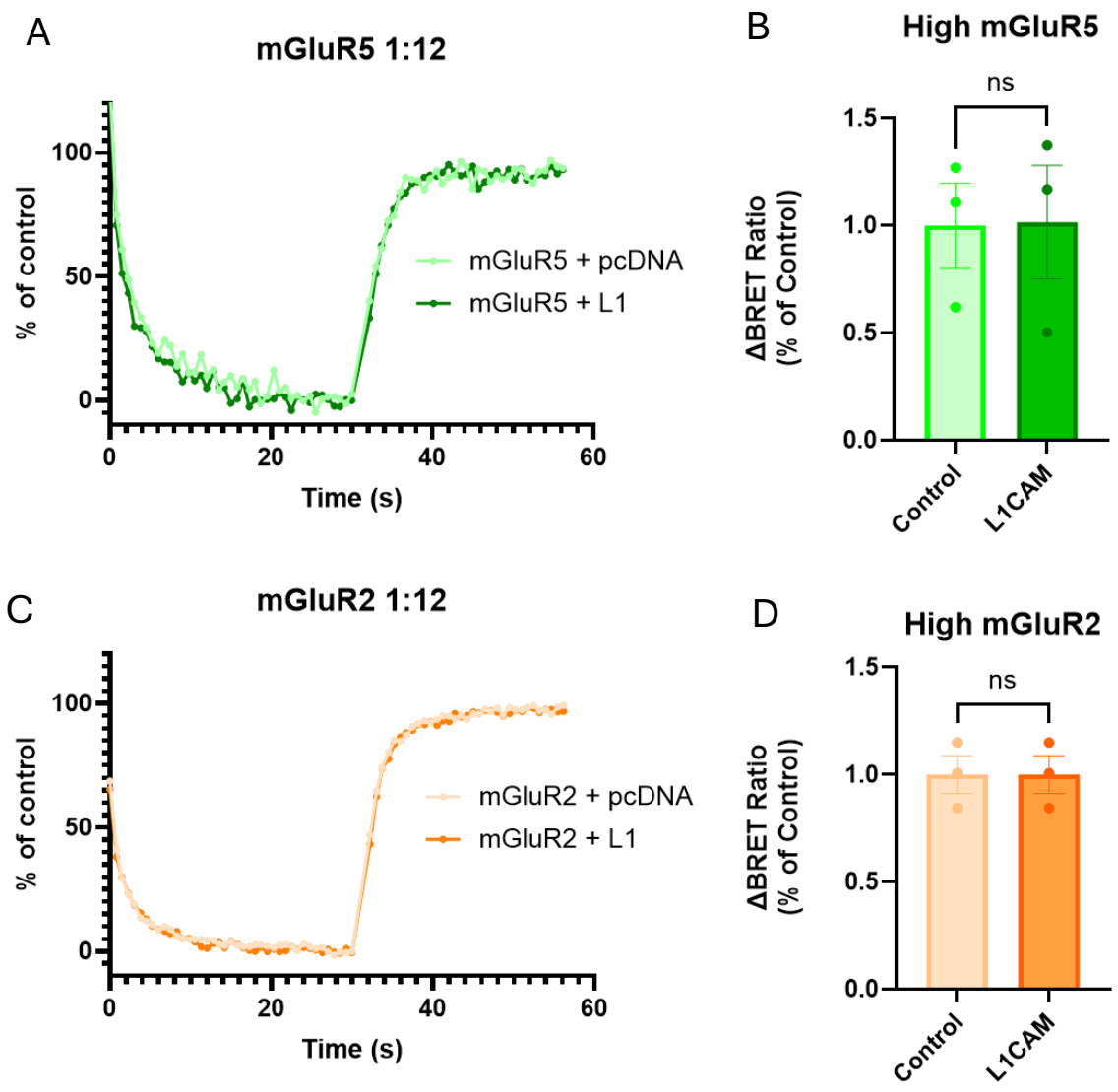

Figure 9. Transcellular interactions between mGluR- and L1CAM-expressing cells at a 1:4 cell ratio, with pcDNA-expressing cells as a control, at the 1:12 DNA ratio of ONE-GO to receptor (n=4). A) Change in BRET ratios between mGluR5-expressing cells cocultured with pcDNA- or L1CAM-expressing cells, calculated as a percent of the control over time. Glutamate injection occurred at 30.0s. B) Quantification of the change in BRET ratio of mGluR5 activation (unpaired t-test). C) Change in BRET ratios between mGluR2-expressing cells cocultured with pcDNA- or L1CAM-expressing cells. D) Quantification of the change in BRET ratio of mGluR2 activation (unpaired t-test).

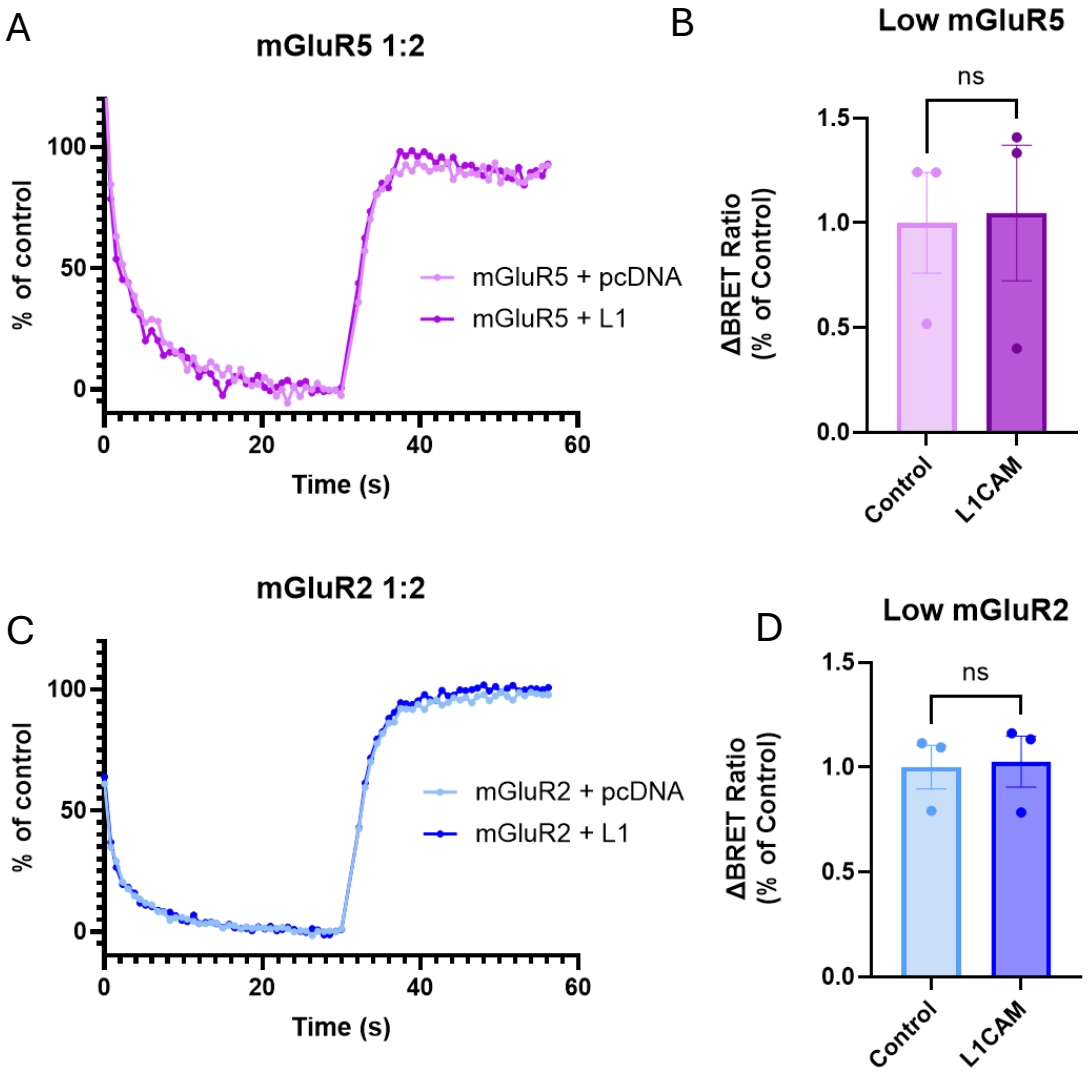

Figure 10. Transcellular interactions between mGluR- and L1CAM-expressing cells at a 1:4 cell ratio, with pcDNA-expressing cells as a control, at the 1:2 DNA ratio of ONE-GO to receptor (n=4 for mGluR5, n=3 for mGluR2). A) Change in BRET ratios between mGluR5-expressing cells cocultured with pcDNA- or L1CAM-expressing cells, calculated as a percent of the control over time. Glutamate injection occurred at 30.0s. B) Quantification of the change in BRET ratio of mGluR5 activation (Mann-Whitney U-test). C) Change in BRET ratios between mGluR2-expressing cells cocultured with pcDNA- or L1CAM-expressing cells. D) Quantification of the change in BRET ratio of mGluR2 activation (unpaired t-test).

References

Alzheimer's Drug Discovery Foundation. 2014. BMS-984923 (ALX-001). Alzheimer's Drug Discovery Foundation. https://www.alzdiscovery.org/uploads/cognitive_vitality_media/BMS-984923_%28ALX-001%29_UPDATE_%28drug_in_development%29.pdf

Beraldo, F. H., Arantes, C. P., Santos, T. G., Machado, C. F., Roffe, M., Hajj, G. N., Lee, K. S., Magalhães, A. C., Caetano, F. A., Mancini, Gabriel. L., Lopes, M. H., Américo, T. A., Magdesian, M. H., Ferguson, S. S. G., Linden, R., Prado, M. A. M., and Martins, V. R. 2011. Metabotropic glutamate receptors transduce signals for neurite outgrowth after binding of the prion protein to laminin γ1 chain. FASEB J., **25**(1), 265–279. https://doi.org/10.1096/fj.10-161653

Beraldo, F. H., Ostapchenko, V. G., Caetano, F. A., Guimaraes, A. L. S., Ferretti, G. D. S., Daude, N., Bertram, L., Nogueira, K. O. P. C., Silva, J. L., Westaway, D., Cashman, N. R., Martins, V. R., Prado, V. F., and Prado, M. A. M. 2016. Regulation of Amyloid β Oligomer Binding to Neurons and Neurotoxicity by the Prion Protein-mGluR5 Complex. J. Biol. Chem., **291**(42), 21945–21955. https://doi.org/10.1074/jbc.M116.738286

Boucard, A. A., Maxeiner, S., and Südhof, T. C. 2014. Latrophilins function as heterophilic cell-adhesion molecules by binding to teneurins: regulation by alternative splicing. J. Biol. Chem. **289**(1), 387–402. https://doi.org/10.1074/jbc.M113.504779

Christaller, W. A. A., Vos, Y., Gebre-Medhin, S., Hofstra, R. M. W., and Schäfer, M. K. E. 2017. L1 syndrome diagnosis complemented with functional analysis of L1CAM variants located to the two N-terminal Ig-like domains. Clin. Genet. **91**(1), 115–120. https://doi.org/10.1111/cge.12763

Christopher, J. A., Aves, S. J., Bennett, K. A., Doré, A. S., Errey, J. C., Jazayeri, A., Marshall, F. H., Okrasa, K., Serrano-Vega, M. J., Tehan, B. G., Wiggin, G. R., & Congreve, M. 2015. Fragment and structure-based drug discovery for a class C GPCR: Discovery of the mGlu5 negative allosteric modulator HTL14242 (3-Chloro-5-[6-(5-fluoropyridin-2-yl)pyrimidin-4-yl]benzonitrile). J. Med. Chem., **58**(16), 6653. https://doi.org/10.1021/acs.jmedchem.5b00892

Conn, P. J., and Pin, J.-P. 1997. Pharmacology and functions of metabotropic glutamate receptors. Annu. Rev. Pharmacol. Toxicol., **37**(1), 205–237. https://doi.org/10.1146/annurev.pharmtox.37.1.205

Dhami, G. K., and Ferguson, S. S. G. 2006. Regulation of metabotropic glutamate receptor signaling, desensitization and endocytosis. Pharm. Ther., **111**(1), 260–271. https://doi.org/10.1016/j.pharmthera.2005.01.008

Dunn, H. A., Patil, D. N., Cao, Y., Orlandi, C., and Martemyanov, K. A. 2018. Synaptic adhesion protein ELFN1 is a selective allosteric modulator of group III metabotropic glutamate receptors in trans. Proc. Natl. Acad. Sci. **115**(19), 5022–5027. https://doi.org/10.1073/pnas.1722498115

Dunn, H. A., Zucca, S., Dao, M., Orlandi, C., and Martemyanov, K. A. 2019. ELFN2 is a postsynaptic cell adhesion molecule with essential roles in controlling group III

mGluRs in the brain and neuropsychiatric behavior. Mol. Psychiatry, **24**(12), 1902–1919. https://doi.org/10.1038/s41380-019-0512-3

Farr, C. D., Gafken, P. R., Norbeck, A. D., Doneanu, C. E., Stapels, M. D., Barofsky, D. F., Minami, M., and Saugstad, J. A. 2004. Proteomic analysis of native metabotropic glutamate receptor 5 protein complexes reveals novel molecular constituents. J. Neurochem. **91**(2), 438–450. https://doi.org/10.1111/j.1471-4159.2004.02735.x

Feng, J., Cai, X., Zhao, J., and Yan, Z. 2001. Serotonin receptors modulate GABA A receptor channels through activation of anchored protein kinase C in prefrontal cortical neurons. J. Neurosci. **21**(17), 6502–6511. https://doi.org/10.1523/JNEUROSCI.21-17-06502.2001

Fourgeaud, L., Bessis, A., Rossignol, F., Pin, J., Olivo-Marin, J., and Hemar, A. 2003. The Metabotropic Glutamate Receptor mGluR5 Is Endocytosed by a Clathrin-independent Pathway. J. Biol. Chem., **278**(14), 12222–12230. https://doi.org/10.1074/jbc.M205663200

Fransen, E., Van Camp, G., D'Hooge, R., Vits, L., and Willems, P. J. 1998. Genotype-phenotype correlation in L1 associated diseases. J. Med. Genet., **35**(5), 399–404. https://doi.org/10.1136/jmg.35.5.399

Haas, L. T., Salazar, S. V., Smith, L. M., Zhao, H. R., Cox, T. O., Herber, C. S., Degnan, A. P., Balakrishnan, A., Macor, J. E., Albright, C. F., and Strittmatter, S. M. 2017. Silent allosteric modulation of mGluR5 maintains glutamate signaling while

rescuing Alzheimer's mouse phenotypes. Cell Rep., **20**(1), 76–88. https://doi.org/10.1016/j.celrep.2017.06.023

Jackson, V. A., Meijer, D. H., Carrasquero, M., van Bezouwen, L. S., Lowe, E. D., Kleanthous, C., Janssen, B. J. C., & Seiradake, E. 2018. Structures of Teneurin adhesion receptors reveal an ancient fold for cell-cell interaction. Nat. Comm., **9**(1), 1079. https://doi.org/10.1038/s41467-018-03460-0

Jin, L. E., Wang, M., Galvin, V. C., Lightbourne, T. C., Conn, P. J., Arnsten, A. F. T., and Paspalas, C. D. 2018. mGluR2 versus mGluR3 metabotropic glutamate receptors in primate dorsolateral prefrontal cortex: postsynaptic mGluR3 strengthen working memory networks. Cereb. Cortex, **28**(3), 974–987. https://doi.org/10.1093/cercor/bhx005

Kiefel, H., Bondong, S., Hazin, J., Ridinger, J., Schirmer, U., Riedle, S., and Altevogt, P. 2012. L1CAM: a major driver for tumor cell invasion and motility. Cell Adhes. Migr., **6**(4), 374–384. https://doi.org/10.4161/cam.20832

Laurén, J., Gimbel, D. A., Nygaard, H. B., Gilbert, J. W., and Strittmatter, S. M. 2009. Cellular prion protein mediates impairment of synaptic plasticity by amyloid-β oligomers. Nature, **457**(7233), 1128–1132. https://doi.org/10.1038/nature07761

Lyonnet, S., Pelet, A., Royer, G., Delrieu, O., Serville, F., Le Marec, B., Gruensteudel, A., Pfeiffer, R. A., Briard, M.-L., Dubay, C., Hors-Cayla, M.-C., Merrer, M. le, and Munnich, A. 1992. The gene for X-linked hydrocephalus maps to Xq28, distal to DXS52. Genomics, **14**(2), 508–510. https://doi.org/10.1016/S0888-7543(05)80254-X

Malik, A. R., and Willnow, T. E. 2019. Excitatory Amino Acid Transporters in Physiology and Disorders of the Central Nervous System. Int. J. Mol. Sci., **20**(22), 5671. https://doi.org/10.3390/ijms20225671

Marín, R., Ley-Martos, M., Gutiérrez, G., Rodríguez-Sánchez, F., Arroyo, D., and Mora-López, F. 2015. Three cases with L1 syndrome and two novel mutations in the L1CAM gene. Eur. J. Pediatr. **174**(11), 1541–1544. https://doi.org/10.1007/s00431-015-2560-2

Martins, V. R., Beraldo, F. H., Hajj, G. N., Lopes, M. H., Lee, K. S., Prado, M. A., and Linden, R. 2010. Prion protein: orchestrating neurotrophic activities. Curr. Issues Mol. Biol., **12**(2), 63. https://doi.org/10.21775/cimb.012.063

Mikulak, J., Negrini, S., Klajn, A., D'Alessandro, R., Mavilio, D., and Meldolesi, J. 2012. Dual REST-dependence of L1CAM: from gene expression to alternative splicing governed by Nova2 in neural cells. J. Neurochem. **120**(5), 699–709. https://doi.org/10.1111/j.1471-4159.2011.07626.x

Otter, M., Wevers, M., Pisters, M., Pfundt, R., Vos, Y., Nievelstein, R. J., and Stumpel, C. 2017. A novel mutation in L1CAM causes a mild form of L1 syndrome: a case report. Clin. Case Rep. **5**(8), 1213–1217. https://doi.org/10.1002/ccr3.1038

Piers, T. M., Kim, D. H., Kim, B. C., Regan, P., Whitcomb, D. J., and Cho, K. 2012. Translational concepts of mGluR5 in synaptic diseases of the brain. Front. Pharmacol. **3**, 199. https://doi.org/10.3389/fphar.2012.00199

Pillai, R. L. I., and Tipre, D. N. 2016. Metabotropic glutamate receptor 5 – a promising target in drug development and neuroimaging. Eur. J. Nucl. Med. Mol. Imaging, **43**(6), 1151–1170. https://doi.org/10.1007/s00259-015-3301-5

Santos, R., Ursu, O., Gaulton, A., Bento, A. P., Donadi, R. S., Bologa, C. G., Karlsson, A., Al-Lazikani, B., Hersey, A., Oprea, T. I., and Overington, J. P. 2017. A comprehensive map of molecular drug targets. Nat. Rev. Drug. Discov. **16**(1), 19–34. https://doi.org/10.1038/nrd.2016.230

Silva, J.-P., Lelianova, V. G., Ermolyuk, Y. S., Vysokov, N., Hitchen, P. G., Berninghausen, O., Rahman, M. A., Zangrandi, A., Fidalgo, S., Tonevitsky, A. G., Dell, A., Volynski, K. E., and Ushkaryov, Y. A. 2011. Latrophilin 1 and its endogenous ligand Lasso/teneurin-2 form a high-affinity transsynaptic receptor pair with signaling capabilities. Proc. Natl. Acad. Sci. **108**(29), 12113–12118. https://doi.org/10.1073/pnas.1019434108

Stachowicz, K., Bobula, B., Kusek, M., Lenda, T., and Tokarski, K. 2021. Evidence for the interaction of COX-2 with mGluR5 in the regulation of EAAT1 and EAAT3 protein levels in the mouse hippocampus. The influence of oxidative stress mechanisms. Brain Res., **1771**, Article 147660. https://doi.org/10.1016/j.brainres.2021.147660

Sun, X., Zhao, Y., and Wolf, M. E. 2005. Dopamine receptor stimulation modulates AMPA receptor synaptic insertion in prefrontal cortex neurons. J. Neurosci. **25**(32), 7342–7351. https://doi.org/10.1523/jneurosci.4603-04.2005

Trivedi, R. R., and Bhattacharyya, S. 2012. Constitutive internalization and recycling of metabotropic glutamate receptor 5 (mGluR5). Biochem. Biophys. Res. Commun., **427**(1), 185–190. https://doi.org/10.1016/j.bbrc.2012.09.040

Um, J. W., Kaufman, A. C., Kostylev, M., Heiss, J. K., Stagi, M., Takahashi, H., Kerrisk, M. E., Vortmeyer, A., Wisniewski, T., Koleske, A. J., Gunther, E. C., Nygaard, H. B., and Strittmatter, S. M. 2013. Metabotropic Glutamate Receptor 5 Is a Coreceptor for Alzheimer Aβ Oligomer Bound to Cellular Prion Protein. Neuron, **79**(5), 887–902. https://doi.org/10.1016/j.neuron.2013.06.036

Vos, Y. J., de Walle, H. E. K., Bos, K. K., Stegeman, J. A., ten Berge, A. M., Bruining, M., van Maarle, M. C., Elting, M. W., den Hollander, N. S., Hamel, B., Fortuna, A. M., Sunde, L. E. M., Stolte-Dijkstra, I., Schrander-Stumpel, C. T. R. M., and Hofstra, R. M. W. 2010. Genotype–phenotype correlations in L1 syndrome: a guide for genetic counselling and mutation analysis. J. Med. Genet. **47**(3), 169–175. https://doi.org/10.1136/jmg.2009.071688

Wang, P., Liao, H., Wang, Q., Xie, H., Wang, H., Yang, M., and Liu, S. 2022. L1 syndrome prenatal diagnosis supplemented by functional analysis of one L1CAM gene missense variant. Reprod. Sci. **29**(3), 768–780. https://doi.org/10.1007/s43032-021-00828-4

Yamasaki, M., Thompson, P., and Lemmon, V. 1997. CRASH syndrome: Mutations in L1CAM correlate with severity of the disease. Neuropediatrics, **28**(3), 175–178. https://doi.org/10.1055/s-2007-973696

Zhou, Y., and Danbolt, N. C. 2014. Glutamate as a neurotransmitter in the healthy brain. *Journal of neural transmission (Vienna, Austria : 1996)*, *121*(8), 799–817. https://doi.org/10.1007/s00702-014-1180-8